JOURNAL OF CATALYSIS **108**, 97–111 (1987)

Methanol and Methane Formation over Palladium Dispersed on the Lanthanide Rare Earth Oxides

M. ALBERT VANNICE,[1] CHAKKA SUDHAKAR, AND MARK FREEMAN

Department of Chemical Engineering, The Pennsylvania State University, University Park, Pennsylvania 16802

Received March 16, 1987; revised May 19, 1987

To complete our study of the effect of the rare earth oxide (REO) support on the CO hydrogenation reaction over Pd, this metal was dispersed on the oxides of the late lanthanide elements—Tb through Lu. The Pd surface area was measured before and after kinetic runs at 0.1 MPa (1 atm) and 1.5 MPa with these Pd/REO catalysts. Methanation activation energies were 30.4 ± 1.1 kcal mole^{-1}, which was virtually the same as that for those determined for the early Pd/REO catalysts. The turnover frequency (TOF) at 548 K for methane ranged from 1.2×10^{-3} to 4.8×10^{-3} s^{-1}, which is up to 40 times that on Pd powder. At 1.5 MPa and 523 K, stable activity was achieved after 48 h on stream and all catalysts showed a selectivity of 83–90% to oxygenates (excluding CO_2), with over 90% of this fraction composed of CH_3OH. The average activation energy for methanol synthesis was 19.6 ± 0.8 kcal mole^{-1}, again nearly identical to values for Pd on the early REOs, and TOFs varied from 1.6×10^{-3} to 6.1×10^{-3} s^{-1}. When these results are combined with those of the previous study (C. Sudhakar and M. A. Vannice, *J. Catal.* **95**, 227 (1985)), the patterns for methanation at 0.1 MPa and CH_3OH synthesis at 1.5 MPa are established as a function of the position of the REO in the periodic table. There is a clear influence of the support on catalytic properties. No trend occurs between methanation activity and the acidity of the support, but a correlation exists between the CH_4 TOF and the activation energy for electrical conductivity, which is consistent with a redox sequence involving oxygen vacancies at the Pd–REO interface which enhance activity by facilitating bond rupture of the CO molecule. The TOF for CH_3OH synthesis shows a strong correlation with the basicity of the REO, which varies with the lanthanide contraction. This behavior also indicated that the support participates directly in the reaction sequence, and this trend strongly supports a mechanism involving formate species on the REO surface, which are formed most readily on the most basic oxides, such as La_2O_3. The possibility of a heterogeneous analog of the Cannizzaro reaction is pointed out, and this route may also influence methanol formation.

INTRODUCTION

Since the initial report by Poutsma *et al.* (*1*) that methanol can be selectively formed over Pd catalysts from CO and H_2, many studies have been conducted on this reaction. There have been two principal reasons for this interest: the large variations in specific activity and selectivity which have been associated with different supports, metal cation promoters, anions in the Pd precursor salt, and Pd crystallite size; and the need for a better understanding of the surface chemistry governing the catalytic sequences in this reaction.

Two of the best supports for methanol synthesis are La_2O_3 (*2, 3*) and Nd_2O_3 (*3–5*); consequently, we decided to undertake a study utilizing each of the lanthanide rare earth oxides (REOs) as a support for Pd. This would allow us to examine the influence on catalytic behavior of certain properties, especially basicity, whose variation is smoothly controlled by the lanthanide contraction. To eliminate any effects due to chloride or hydrolysis of the REO, all catalysts were prepared with diammine Pd nitrite using a nonaqueous impregnation

---

[1] To whom correspondence should be addressed.

0021-9517/87 $3.00

method (*6*). An earlier report described the behavior of Pd dispersed on the first half of the REO series—La through Eu (*3*). This paper concludes the study, unifies the results for this family of Pd/REO catalysts, and discusses the implications of the observed correlations on the various reaction mechanisms that have been proposed for both CH_4 and CH_3OH synthesis.

EXPERIMENTAL

Catalyst Preparation

The late rare earth oxide (REO) supports used in this study were terbium oxide, Tb_4O_7; dysprosium oxide, Dy_2O_3; holmium oxide, Ho_2O_3; erbium oxide, Er_2O_3; thulium oxide, Tm_2O_3; ytterbium oxide, Yb_2O_3; and lutetium oxide, Lu_2O_3. These and the early REOs in the previous study (*3*) were obtained from the Sigma Chemical Co. and each had a reported purity of 99.9%. The bulk oxide phases were confirmed by X-ray diffraction measurements. As supplied by the manufacturers, these late REOs had low surface areas of 1 to 11 m^2/g, and a hydrolysis procedure followed by calcination in flowing air at 773 K was again employed to increase surface area (*6*). However, this treatment produced little or no increase in surface area, a result ascribed to the lanthanide contraction which decreases basicity and renders the oxides less susceptible to hydrolysis (*7, 8*).

To prevent any hydrolysis of the REO during the impregnation step, the 1.5 wt% Pd/REO catalysts were prepared by a nonaqueous, multiple-incipient wetness technique using diammine palladium(II) nitrite, $Pd(NH_3)_2(NO_2)_2$ (Alfa Products, Ventron Corp.) dissolved in *N,N*-dimethylformamide (DMF), $HCON(CH_3)_2$ (Spectro ACS grade, Eastman–Kodak Co.). Details are given elsewhere (*6*). The Pd/REO catalysts were then dried in air at 388 K overnight, calcined at 773 K for 2 h under 450 cc/min air (Airco, grade zero), and stored in a desiccator.

Adsorption Measurements

Hydrogen and carbon monoxide chemisorption at 300 K as well as BET measurements were performed in a glass high-vacuum system capable of an ultimate vacuum below 10^{-6} Torr. A Texas Instrument Model 145 precision pressure gauge was used to measure gas pressures during adsorption isotherms. Details have been given elsewhere (*9*). The method of Benson *et al.* (*10*) was used to measure both the hydrogen chemisorbed on the Pd surface and that absorbed to form the bulk β-hydride phase. The technique of Yates and Sinfelt (*11*) was used to measure irreversible CO chemisorption. For initial chemisorption measurements after a low-temperature reduction (LTR) at 573 K and a high-temperature reduction (HTR) at 773 K, the same sample was employed. The sequence of experiments was the same as that used previously (*3*). Each Pd/REO catalyst was also characterized by H_2 and CO chemisorption after its use in the kinetic studies. The same sequence of adsorption measurements was again followed.

Kinetic Studies

The kinetic studies at 1 atm were performed in a glass differential plug–flow microreactor which has been described previously (*5*). Total conversions were kept below 5% to eliminate heat and mass transfer effects, as confirmed by application of the Weisz criterion (*12*). To minimize complications due to catalyst deactivation, a bracketing technique was employed which consisted of alternate 20-min cycles of feed gas and pure hydrogen (*13*). Both ascending and descending temperature studies were conducted to check for any catalyst deactivation.

The high-pressure kinetic studies were performed in a stainless-steel system utilizing a reactor passivated by gold-plating to render it inactive, Brooks mass flow controllers, a Grove Mity Mite SD-91W back pressure regulator, and a digital pressure

TABLE 1

Initial Uptakes on Fresh 1.5% Pd/REO Catalysts after an LTR Reduction at 573 K

Catalyst	BET surface area of REO ($m^2\ g^{-1}$)	Chemisorption (μmole/g)		$CO_{(a)}/H_{(a)}$	Bulk hydride ratio[a] (H_b/Pd_b)	Percentage Pd exposed[b]	Average Pd[c] crystallite size (nm)
		H_2	CO				
Pd/Tb_4O_7	2.5	4.5	8.2	0.91	0.61	6.4	18
Pd/Dy_2O_3	10.7	20.1	43.6	1.1	0.57	28.5	4.0
Pd/Ho_2O_3	3.4	10.6	23.2	1.1	0.54	15.0	7.5
Pd/Er_2O_3	5.3	7.3	15.8	1.1	0.54	10.4	11
Pd/Tm_2O_3	1.4	4.1	4.5	0.55	0.61	5.8	19
Pd/Yb_2O_3	2.7	5.5	10.4	0.95	0.63	7.8	14
Pd/Lu_2O_3	2.0	5.1	8.5	0.83	0.58	7.2	16

[a] H_b = H atoms absorbed; $Pd_b = Pd_{total} - Pd_{surface}$.

[b] $H_{(ad)}/Pd_{total} \times 100$.

[c] See Ref. (*20*).

transducer from Validyne Corp. The reactor effluent was analyzed using a Perkin-Elmer Sigma 2B gas chromatograph with temperature programming and Chromosorb 106 columns. Additional details have been given elsewhere (*3*). After an LTR at 573 K, all catalysts required about 45 h to reach steady-state operation at 523 K. After this period both ascending and descending Arrhenius plots were acquired between 490 and 530 K. Approximately 45 min was required for stabilization at each temperature. Total CO conversions were kept below 1% at 523 K to prevent diffusional limitations and to allow CH_3OH synthesis to be considered an irreversible reaction.

RESULTS

Chemisorption

Initial hydrogen and carbon monoxide uptakes on the fresh Pd/REO catalysts are presented in Table 1 after a low-temperature reduction at 573 K, and adsorption results for the used catalysts after CO hydrogenation at 1.5 MPa (14.6 atm) are presented in Table 2. Most of the fresh catalysts exhibited relatively low-percentage Pd exposures, ranging from 6.4% for Pd/Tb_4O_7 to 28.5% for Pd/Dy_2O_3, which is at least partially attributable to the low surface area of the REO supports. The bulk hydride ratios, H_b/Pd_b, were near the value of 0.6 expected for normal β-hydride formation, and the CO_{ad}/H_{ad} ratios were near unity for all catalysts, except Pd/Tm_2O_3, as anticipated for clean Pd surfaces (*14*). During the kinetic runs at 1.5 MPa, a significant loss of available Pd surface area occurred, as shown in Table 2; however, with the exception of Pd/Dy_2O_3, all bulk hydride and H_{ad}/CO_{ad} ratios appeared quite normal. A high-temperature reduction alone also markedly decreased uptakes of CO and H_2 but, in contrast, the hydride ratios dropped to 0.4–0.5 and the CO_{ad}/H_{ad} ratios frequently climbed to values between 5 and 8 (*15*). These two results strongly imply the partial reduction and migration of REO species onto the Pd surface, which cannot only encapsulate some crystallites, thereby preventing hydride formation and giving low bulk hydride ratios, but also produce sites for irreversible CO adsorption on the support. Similar behavior has been reported previously for La and other REOs (*5, 14, 16, 17*), and it complicates any calculation of crystallite size from the uptake data, especially since no Pd X-ray diffraction peaks were detected for any of these catalysts, new or used. However, the hydrogen uptakes should still be a valid measure of Pd

TABLE 2

Uptakes on Used 1.5% Pd/REO Catalysts after Reaction at 14.6 atm (LTR Pretreatment)

Catalyst	Chemisorption (μmole/g)		$CO_{(a)}/H_{(a)}$	Bulk hydride ratio (H_b/Pd_b)	Percentage Pd exposed (H_b/Pd_b)
	H_2	CO			
Pd/Tb_4O_7	4.4	7.8	0.89	0.65	6.2
Pd/Dy_2O_3	3.7	5.8	0.79	0.45	5.2
Pd/Ho_2O_3	2.8	6.3	1.1	0.55	4.0
Pd/Er_2O_3	2.1	4.9	1.2	0.61	3.0
Pd/Tm_2O_3	1.1	2.4	1.1	0.62	1.6
Pd/Yb_2O_3	2.3	5.4	1.2	0.70	3.3
Pd/Lu_2O_3	1.9	4.9	1.3	0.63	2.7

surface atoms accessible to the reactants; therefore, the turnover frequency (TOF) is based on the initial H adsorption for the first runs in the kinetic sequence at 0.1 MPa (1 atm) and on the H adsorption on the used samples for the final runs in the sequence at 1.5 MPa.

Kinetic

Kinetic parameters obtained at 1 atm are shown in Table 3. All catalysts showed some deactivation during the ascending–descending temperature cycle, as shown in Fig. 1. An extended analysis of one catalyst required four ascending–descending cycles before the activity stabilized, but the average activation energy for each cycle was nearly constant. Consequently, the average activation energies and TOF values listed in Table 3 should be very representative for the stable catalysts.

The activation energy for CH_4 formation was nearly constant at 30.4 kcal $mole^{-1}$ with an average deviation from the mean of 1.1 kcal $mole^{-1}$, while the average activation energy for CO_2 was 23 kcal/mole. The

TABLE 3

Kinetic Behavior of CO Hydrogenation over 1.5% Pd/REO Catalysts (LTR Pretreatment, $T = 548$ K, $P = 0.1$ MPa, $H_2/CO = 3$)

Catalyst	Activity (μmole $\cdot$ s^{-1} $\cdot$ g^{-1} $\times$ 10^3)		TOF[a] (s^{-1} $\times$ 10^3)			Activation energy (kcal/mole)	
	CH_4	CO_2	CH_4[b]	CH_4	CO_2	CH_4	CO_2
Pd/Tb_4O_7	42.8	34.1	1.3	4.8	3.8	29.5	24.5
Pd/Dy_2O_3	77.2	82.8	0.47	1.9	2.1	31.8	25.0
Pd/Ho_2O_3	34.3	35.0	0.43	1.6	1.6	30.0	24.8
Pd/Er_2O_3	23.2	16.4	0.42	1.6	1.1	30.6	25.3
Pd/Tm_2O_3	9.7	11.1	0.31	1.2	1.4	30.6	19.6
Pd/Yb_2O_3	30.8	23.1	0.80	2.8	2.1	28.6	23.7
Pd/Lu_2O_3	14.0	22.7	0.35	1.4	2.2	31.8	22.2

[a] Based on H_2 chemisorbed on fresh sample (Table 1).

[b] Value at 523 K.

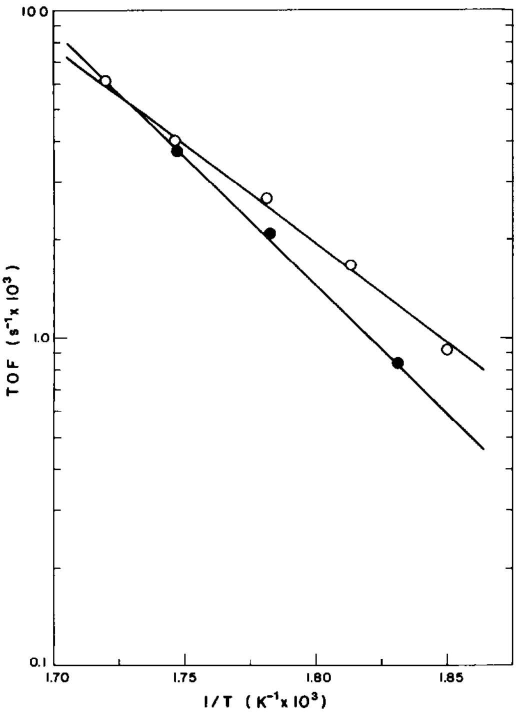

FIG. 1. Arrhenius plot for methane turnover frequency, TOF, on 1.5% Pd/Tm_2O_3 at $P = 0.1$ MPa and $H_2/CO = 3$. Ascending temperature (○); descending temperature (●).

range of the specific activity for CH_4 formation over Pd dispersed on the late REO supports was small, showing a four-fold variation. Methane formation was highest on Tb_4O_7-supported Pd with a second peak for Pd/Yb_2O_3. No oxygenate formation was observed at 0.1 MPa on any of these Pd/REO catalysts except for Pd/Dy_2O_3, which had a selectivity to CH_3OH of approximately 50% at 503 K. After an HTR pretreatment at 773 K, these catalysts exhibited large losses in activity per gram although TOF values were very similar (*15*), again indicating a large loss of available Pd surface area due to sintering and/or encapsulation. The near independence of the CH_4 activity on total pressure is in excellent agreement with the results reported recently by Hicks and Bell for Pd/La_2O_3 (*18*).

The kinetic studies at 1.5 MPa were performed after an LTR pretreatment only. The change in activity with time on stream was similar for all catalysts, with the rate of deactivation decreasing with time before stabilization was attained after 40 to 45 h. A typical activity maintenance plot is shown in Fig. 2. The steady-state CH_3OH activity was typically 30 to 50% of the rate measured after 1 h on stream, while CH_4 deactivation was somewhat less severe and CO_2 decreased more significantly. Table 4 presents a comparison of the ratios of steady-state activity to initial activity for

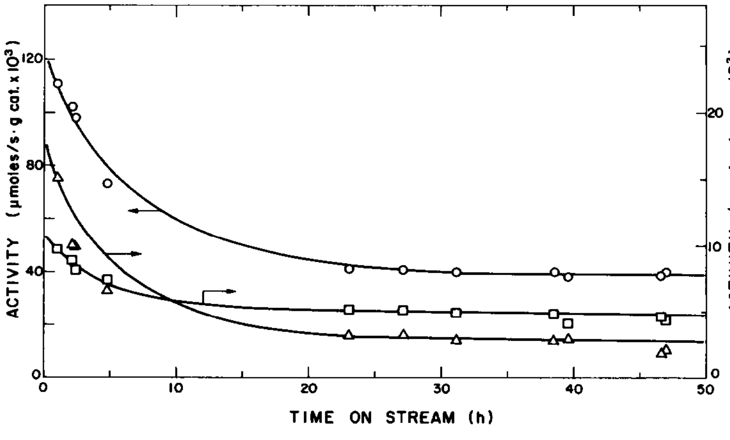

FIG. 2. Activity maintenance for CO hydrogenation over 1.5% Pd/Dy_2O_3 at $P = 1.5$ MPa, $T = 523$ K, and $H_2/CO = 3$. CH_3OH (○); CH_4 (□); CO_2 (△).

TABLE 4

Changes in Activity and Chemisorption Capacity with Time on Stream (T = 523 K, 1.5 MPa, H_2/CO = 3)

Catalyst	Ratio of activity[a] steady-state/ initial			Ratio of Chemisorption used catalyst/ fresh catalyst	
	CH_3OH	CH_4	CO_2	H_2	CO
Pd/Tb_4O_7	0.53	0.43	0.22	0.98	0.91
Pd/Dy_2O_3	0.34	0.53	0.22	0.19	0.13
Pd/Ho_2O_3	0.29	0.50	0.26	0.26	0.27
Pd/Er_2O_3	0.36	0.67	0.33	0.29	0.31
Pd/Tm_2O_3	0.29	0.45	0.24	0.27	0.53
Pd/Yb_2O_3	0.42	0.59	0.31	0.42	0.53
Pd/Lu_2O_3	0.45	0.48	0.31	0.37	0.59

[a] Initial activity defined as that after 1 h on stream; steady-state activity obtained after 44–48 h on stream.

CH_4, CH_3OH, and CO_2 formation along with the ratios of the chemisorption on the used and fresh samples. The strong parallel between the changes in CH_3OH activity and the chemisorption capacity again indicates that loss of available Pd surface area is primarily responsible for the decrease in CH_3OH synthesis.

Table 5 describes the kinetic behavior under steady-state conditions at 1.5 MPa and 523 K. The activation energies for both CH_3OH and CH_4 formation are very consistent across the series with an average value of 19.6 ± 0.8 kcal/mole for CH_3OH formation and 34.0 ± 1.6 kcal/mole for CH_4 formation.

The CH_3OH activity varied by a factor of 6 among the catalysts, from 5.9×10^{-9} mol s^{-1} g cat^{-1} for Pd/Lu_2O_3 to 38×10^{-9} mol s^{-1} g cat^{-1} for Pd/Tb_4O_7, while the CH_4 ac-

TABLE 5

Kinetic Behavior of CO Hydrogenation over 1.5% Pd/REO Catalysts (LTR Pretreatment, T = 523 K, P = 1.5 MPa, H_2/CO = 3)

Catalyst	Activity (μmole · s^{-1} · g^{-1} × 10^3)			TOF[a] (s^{-1} × 10^3)			Activation energy (kcal/mole)			Percentage oxygenates in organic products[b]	Percentage DME in oxygenates (mole%)
	CH_3OH	CH_4	CO_2	CH_3OH	CH_4	CO_2	CH_3OH	CH_4	CO_2		
Pd/Tb_4O_7	20.6	3.5	2.1	2.4	0.40	0.24	19.6	31.2	16.4	87	0.8
Pd/Dy_2O_3	37.9	5.1	3.3	5.1	0.69	0.45	18.4	32.1	15.2	90	—
Pd/Ho_2O_3	19.1	3.1	2.3	3.4	0.55	0.41	19.2	35.4	17.0	88	3
Pd/Er_2O_3	25.4	3.8	2.3	6.1	0.90	0.56	18.9	35.1	19.5	90	4
Pd/Tm_2O_3	7.4	1.9	1.2	3.4	0.88	0.56	19.2	34.6	16.5	84	8
Pd/Yb_2O_3	14.1	3.3	2.0	3.1	0.73	0.44	20.8	33.3	15.0	83	5
Pd/Lu_2O_3	5.9	1.3	1.7	1.6	0.34	0.45	21.1	36.4	26.1	88	10

[a] Based on $H_{(a)}$ on used LTR samples (Table 2).

[b] Carbon atom basis.

tivity exhibited a four-fold variation. A comparison of the CH_3OH TOF values at 523 K showed a smaller fourfold variation while the CH_4 TOFs changed by a factor of 3. Small amounts of ethane and dimethyl ether (DME) were detected; however, the selectivity to oxygenates, based on moles CO converted, was high for all catalysts and ranged between 83 and 90%, as shown in Table 5.

DISCUSSION

Under conditions thermodynamically unfavorable for CH_3OH synthesis, Pd dispersed on Al_2O_3 was originally found to have a moderate specific activity for CO conversion to CH_4 (*13*), but for unsupported Pd or Pd dispersed on SiO_2, the turnover frequency for methanation was one to two orders of magnitude lower (*19*). A subsequent study by Poutsma *et al.* reported that at higher pressures Pd was an active and quite selective CH_3OH synthesis catalyst (*1*). This important discovery led to numerous investigations to better understand the catalytic chemistry associated with CO/H_2 reactions over Pd. However, there is currently no universal agreement about either the principal reaction paths or the means by which different variables alter reaction rates. To address these topics, this discussion is divided into two sections—the first deals with reaction sequences for methanation, and the last discusses models for CH_3OH formation over Pd dispersed on REOs and other supports.

Methanation

Careful studies of Pd catalysts have shown that the support can significantly enhance the TOF for methanation over Pd at both 1 atm (*3, 5, 19, 20*) and higher pressures (*2, 3, 21*). At 1 atm and near-stoichiometric feeds, Pd blacks and powders have a low TOF value near $0.12 \times 10^{-3}\ s^{-1}$ which increases to between 0.2 and $0.9 \times 10^{-3}\ s^{-1}$ at 10–15 atm. (All CH_4 activities are at 548 K unless otherwise noted.) Dispersing Pd on SiO_2 typically gives only small TOF enhancements, if any, with values ranging from 0.1 to $1 \times 10^{-3}\ s^{-1}$ (*18–24*) although higher values are infrequently reported (*23, 25*). However, Al_2O_3 routinely gives an order of magnitude increase in TOF (*19, 20, 26*), and other supports such as TiO_2 and CeO_2 can increase the rate even more (*2, 3, 20, 21*).

There has been an evolution of reaction models describing methanation over the noble metals (*27, 28*). In one of the more recent, we proposed a reaction sequence invoking H-assisted C–O bond rupture as the rate-determining step (rds) (*20*), and subsequent studies by Mori *et al.* (*26*) and Rieck and Bell (*29*) have provided additional evidence that adsorbed hydrogen interacts with the CO molecule in an rds. Shortly thereafter, a number of investigators proposed that the support itself could be directly involved, with its role being that of facilitating CO bond rupture (*24, 30–32*). These roles for both the hydrogen and the support are consistent with the knowledge that CO dissociation on clean bulk Pd does not occur readily (*33*). A review of the literature reveals a wide range of activation energies for methanation, varying from 14 kcal $mole^{-1}$ for some Pd/Al_2O_3 catalysts (*19, 26*) to over 40 kcal $mole^{-1}$ for La-promoted Pd/SiO_2 (*34*), and it has already been suggested that at least two reaction pathways exist (*3*)—one involving CO dissociation on certain Pd sites whose concentration may be enhanced on very small crystallites (*25*) and another allowing the activation of the CO bond via electron transfer between the oxygen end of the molecule and a site on the support such as a Lewis acid (*24*) including an exposed metal cation (*3, 31*). We believe the results reported here provide strong support for the latter concept.

If the methanation TOF values in Table 3 are combined with those reported in Ref. (*3*), the pattern of methanation activity can be established as a consequence of the position of the REO support in the periodic table. It is illustrated in Fig. 3 along with

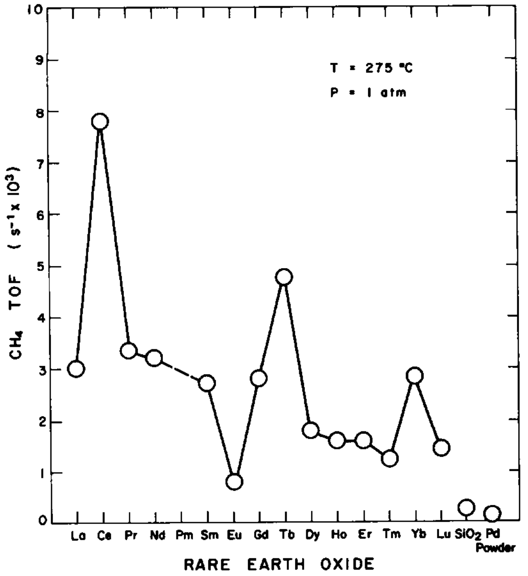

FIG. 3. Variation of methane turnover frequency on Pd with REO support: $P = 0.1$ MPa, $T = 548$ K, $H_2/CO = 3$. Values for 2.33% Pd/SiO_2 and Pd powder from Refs. (*20*) and (*3*), respectively.

typical TOF values for Pd on SiO_2 and unsupported Pd for comparison. This behavior can be summarized as follows: (1) For most of the Pd/REO catalysts there is a steady, almost linear decrease in activity as the RE atomic number increases; (2) superimposed on this trend are maxima at the oxides of Ce, Tb, and Yb and a minimum at Eu oxide; and (3) all REO-supported Pd catalysts have higher TOFs than SiO_2-supported Pd or unsupported Pd. Clearly the REO plays an intrinsic role in this 10-fold variation in TOF. These results do not correlate with the increase in acidity due to the lanthanide contraction (*35*), which tends to argue against an electronic promoter effect on the Pd (*16, 36*). However, we have found an intriguing correlation between the TOF and the activation energy for electrical conductivity using reported literature values (*37, 38*), as shown in Fig. 4. This trend may be purely fortuitous; on the other hand, it may provide some insight into the role of the support in increasing the rate of methanation. The implication of the trend in Fig. 4 is very consistent with the model proposed earlier (*3*) in which we associated the higher specific activity on Pd/REO catalysts to a pathway involving the interaction of CO with a lanthanide rare earth metal (Ln) cation via a redox sequence; for example,

---

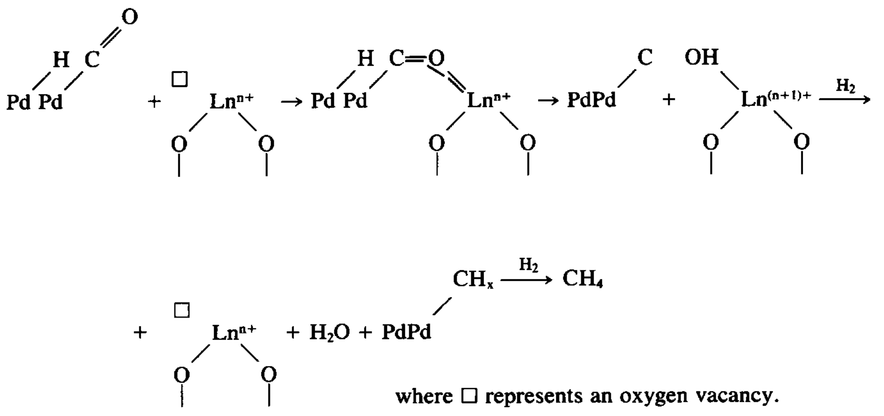

where □ represents an oxygen vacancy.

Nonstoichiometry is commonplace among the REOs under low oxygen pressures or reducing conditions, and removal of oxygen from the lattice produces vacancies and *n*-type semiconductivity (*65*). The activation energy for electrical conductivity

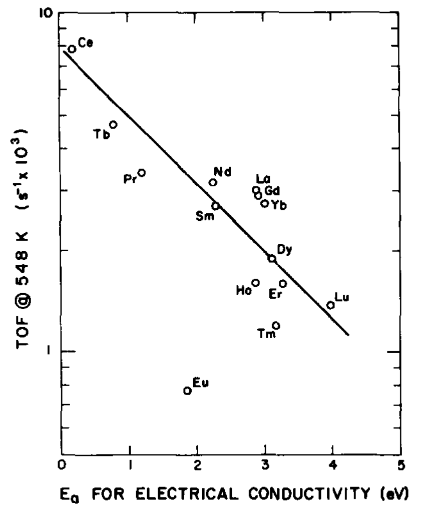

FIG. 4. Correlation of CH_4 turnover frequency on Pd with the activation energy for electrical conductivity in the REO support: $P = 0.1$ MPa, $T = 548$ K, $H_2/CO = 3$.

reflects the ease with which oxygen can be removed and the electrons can be transported through the solid; consequently, the number of vacancies will be dependent upon this value. The similarity in the activation energy for CH_4 formation at 0.1 MPa over all the Pd/REO catalysts—31.2 ± 1.0 kcal $mole^{-1}$—indicates that the rate enhancement is due to an increase in the preexponential factor, most likely an increase in active site density. We would like to suggest that the new active sites in the metal–support interface region are oxygen vacancies, which can facilitate the methanation reaction by dissociating CO via a redox sequence, as shown above. Their concentration and their activity are governed by the activation energy for conductivity thereby providing the correlation in Fig. 4, but the former variable is presumed to be the more important one. Although there is uncertainty about the actual oxides that exist under our reaction conditions, the resistivity measurements of Bogoroditskii *et al.* (*37*) on *n*-type semiconducting REOs provided linear Arrhenius plots between 300 and 1600 K; therefore, these data should provide a reasonable approximation of the relative ease of oxygen vacancy formation. Eu is the only REO with an expected 2+ valence state due to the stability of its half-filled shell, and this factor may explain why Eu does not follow the trend in Fig. 4. This redox sequence should be applicable to other supports which have oxygen vacancies and/or Lewis acid sites at the surface, such as TiO_2 and Al_2O_3, and its presence could explain the higher rates of methanation with these oxides (*24, 30, 31*).

The Pd–support interface region is obviously very important in this model and its optimization is needed for highest activity. Extremely small Pd clusters and crystallites might be expected to maximize the metal–support interface, but recent studies have provided clear evidence that under reducing conditions many supports such as TiO_2 (*36, 39–42*), La_2O_3 (*14, 16, 17*), and the REOs (*5*) can migrate onto the surface of the dispersed metal particles; therefore, high dispersions are not required to achieve a large interface area relative to the available Pd surface. In conclusion, we believe that, depending on its surface chemical properties, the support can be an important participant in the methanation reaction, and it assists by providing interfacial sites which facilitate C–O bond rupture of a CO molecule adsorbed on the metal (i.e., Pd). Consequently, both the type of site and the site density on the support will affect the rate when normalized to the number of available metal surface atoms.

Methanol Synthesis

Although CH_3OH can be formed with reasonable selectivity over unsupported Pd at 10–15 atm, the turnover frequency is very low (*2, 3*), but dispersing Pd on essentially any support has increased its specific activity, and a choice of the proper support has provided very selective catalysts with a high methanol TOF under thermodynamically favorable conditions (*1–4, 18, 21, 24, 43–46*). In addition, promoters such as the Group I and Group II metals have also been found to increase the rate of CH_3OH formation (*47–52*), it has been claimed that Pd crystallite size can alter selectivity (*25*), and the Pd precursor compound can affect catalytic behavior (*2, 43*) with a positive role being attributed to the chloride ion (*43*). This situation is further complicated by the fact that even different silicas can produce markedly different behavior (*24, 43*).

Our understanding of the chemistry associated with CH_3OH formation is not yet sufficient to explain either this plethora of parameters or the wide variation in catalytic behavior reported in the literature. A number of general models have been forwarded to describe the reaction pathway. Poutsma *et al.* (*1, 33*) suggested that adsorbed CO and hydrogen react to form a CH_xO intermediate, as did Fajula *et al.* (*24*). Ponec and co-workers (*4, 45, 50*) have proposed that Pd^{n+} ions are required for CH_3OH synthesis. Tamaru and co-workers (*47, 48*) first proposed that formate species created on the support were important intermediates and they provided strong IR evidence in support of this. Since then others have also identified formate intermediates using IR spectroscopy (*53*), and chemical trapping techniques have provided evidence for formate, formyl, and methoxy species on supported Pd catalysts (*46, 49, 54*), with the last investigation emphasizing REO supports. Also, it has been found that certain oxides such as La_2O_3 can form CH_3OH in the absence of Pd (*55, 56*), which has led to the suggestion that a bifunctional catalytic reaction may occur (*55*). Finally, thorough studies by Bell and co-workers (*44, 57*) have shown only a small, three-fold variation in the CH_3OH TOF over the Pd (111) plane compared to the Pd (100) plane.

Activation energies for CH_3OH have not been frequently reported, but they have ranged from 14 to 20 kcal $mole^{-1}$ for SiO_2-supported Pd (*2, 18, 21, 48*), from 14 to 22 for Pd on MgO, ZnO, Al_2O_3, TiO_2, ZrO_2, and SiO_2–Al_2O_3 (*2, 21*), and from 13 to 21 for La_2O_3-supported Pd (*2, 3, 18, 58*). For the Pd/REO catalysts studied here and previously (*3*), the activation energy is quite invariant with a mean value and standard deviation of 19.1 ± 1.0 kcal $mole^{-1}$. Under reaction conditions of 1.6 MPa, 532 K, and an H_2/CO ratio of 2.3, Lunsford and co-workers (*43*) reported TOF values on Pd/SiO_2 varying from 0.6 to 42×10^{-3} s^{-1}, depending on Pd percentage exposure and type of silica. Under very similar conditions, Hicks and Bell (*18*) reported a TOF of 3×10^{-3} s^{-1} over a Pd/SiO_2 catalyst (21% Pd exposed), and Berube *et al.* (*21*) reported a value of 2.4×10^{-3} s^{-1} for 2.33% Pd/SiO_2 (12% Pd exposed). The use of La_2O_3 or Nd_2O_3 has resulted in large increases in the CH_3OH TOF (*2, 3, 18*) with the highest reported value being 99×10^{-3} s^{-1} for a Ventron 0.2% Pd/La_2O_3 catalyst (*2*) while a 1.9% Pd/La_2O_3 catalyst (16% exposed) and a 1.5% Pd/La_2O_3 catalyst (6% exposed) had very similar TOFs at 1.5 MPa and 523 K of 20 and 13.4×10^{-3} s^{-1}, respectively (*3, 18*). The very high TOFs over Pd on Davison 57 and 59 silicas (*2, 43, 52*), compared to other types of SiO_2, have not yet been explained. Kelly *et al.* (*43*) found that the addition of Li to their Pd/SiO_2 catalysts increased the CH_3OH TOF, but the amount required for significant activity enhancement was so large that it appeared to eliminate impurities as an explanation.

The activity pattern obtained for CH_3OH synthesis over Pd/REO catalysts under a standard set of conditions is shown in Fig. 5 along with TOF values on SiO_2-supported Pd and Pd powder for comparison. There is a general trend that the TOF decreases with an increase in the RE atomic number and hence with the lanthanide contraction. This contraction decreases the basicity of the oxides across the row, and if the cationic radius can be taken as a measure of basicity (*35*), the TOF is highest on the most basic supports, in agreement with previous findings. This is demonstrated more clearly in Fig. 6. Because the Pr_6O_{11} and Tb_4O_7 have mixed valencies, the radii listed are stoichiometric averages of the +3 and +4 states; in addition, because of the stable $4f^0$ configuration of Ce^{4+}, CeO_2 has been reported to be the least basic of the REOs and in actuality it should be to the left of Lu on a basicity scale (*59*), as indicated in the figure.

We interpret these results as additional evidence that (1) the support can noticeably enhance CH_3OH synthesis; (2) the greater the basicity, the greater the rate increase; and (3) the support is directly involved in the synthesis, as demonstrated by oxygen isotopic exchange studies (*47*).

We have already argued in favor of the possibility of two routes for CH_3OH synthesis (*3*), as suggested by Kiennemann and co-workers (*46, 49*). One is through a formyl intermediate associated primarily with the Pd surface, and the other is through a formate species that can be formed from the migration of a formyl species from the Pd to the support (*48, 53*) or by CO insertion into hydroxyl groups on the support

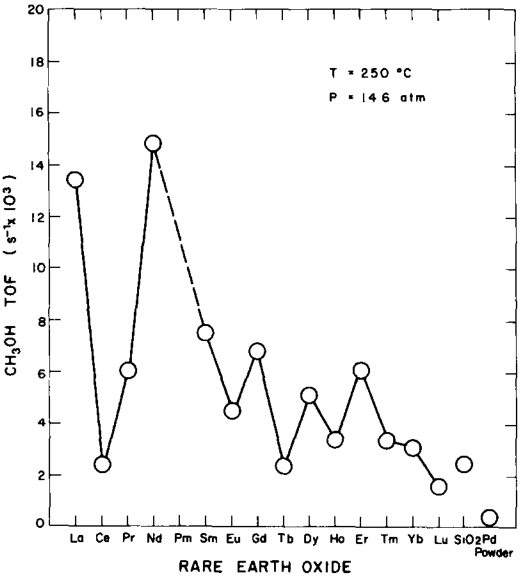

FIG. 5. Variation of CH_3OH turnover frequency on Pd with REO support: P = 1.5 MPa, T = 523 K, H_2/CO = 3. Values for 2.33% Pd/SiO_2 and Pd powder from Refs. (*20*) and (*3*), respectively.

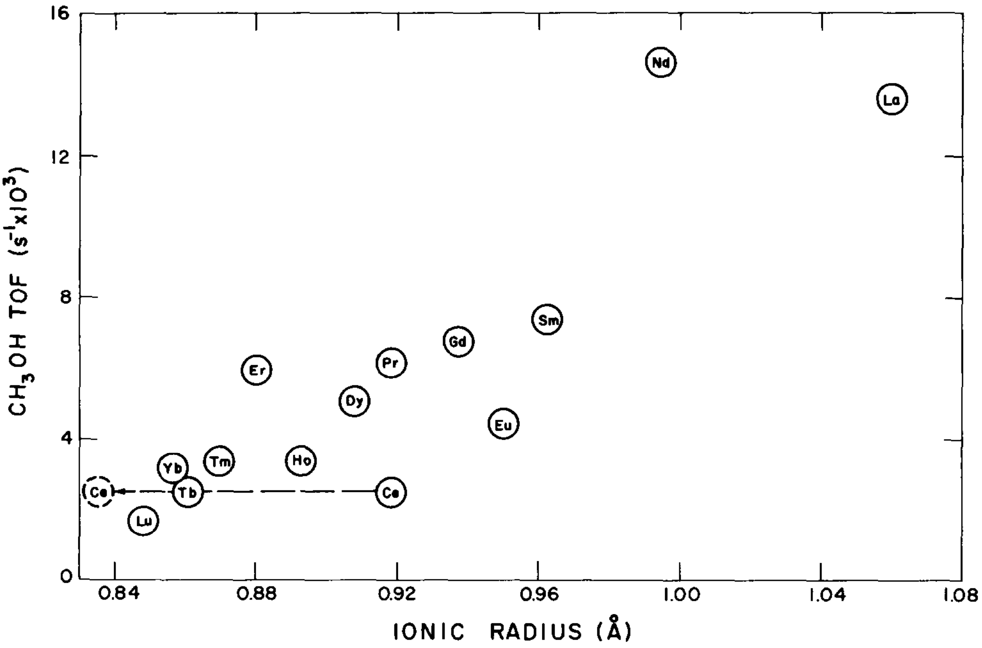

FIG. 6. Correlation of methanol turnover frequency on Pd with basicity of REO support as represented by the lanthanide contraction: P = 1.5 MPa, T = 523 K, H_2/CO = 3.

surface (*49, 55, 60, 61*). The subsequent hydrogenation of the formate species through a methoxy intermediate is a reasonable pathway and has been supported by a number of studies (*47–49, 53, 55, 60, 62*). We favor a model invoking formate intermediates created at additional sites on the oxide support, and believe these results are consistent with such a mechanism. Further support for this argument is given by a comparison of available thermodynamic data describing the formation of the bulk formates and acetates from the corresponding REOs (*63, 64*), as listed in Table 6. The heats of formation of the formates parallel those of the acetates, which exhibit a decrease in free energy of formation as basicity decreases; we consequently expect the same trend to exist for the free energies associated with the RE formates.

A marked enhancement in CH_3OH activity has repeatedly been reported upon the addition of strong bases to Pd catalysts (*43, 45, 47–52*). As a result, we would like to suggest here a possible additional synthesis route involving formyl and formate species that could operate *concurrently* with those proposed previously. It constitutes a heterogeneous analog to the homogeneous Cannizzaro reaction, as illustrated below for formaldehyde:

$$2\,HCHO + \text{strong base } (OH^-) \rightarrow HCOO^- + CH_3OH.$$

The hydrogenation of the surface formate species would complete the catalytic cycle. For Pd on a lanthanide (Ln) REO, a possible sequence is

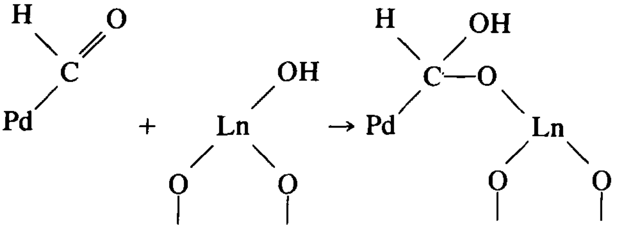

[1]

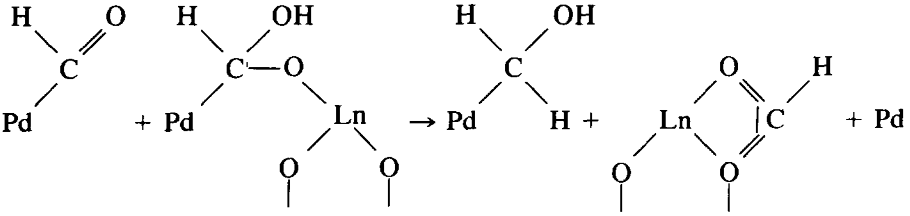

[2]

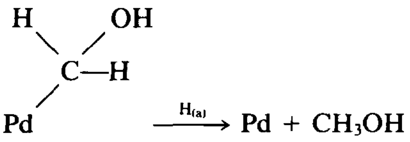

[3]

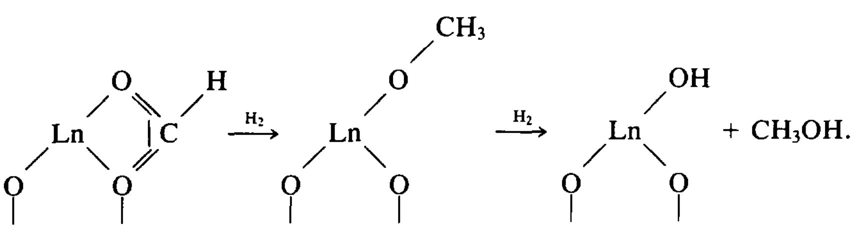

[4]

TABLE 6

Standard Enthalpies and Free Energies of Formation of Lanthanide (Ln) Rare Earth Formates and Acetates from the Oxides According to the Reactions Below[a]

REO (Ln_2O_3)	ΔH_1 (kJ/mole)	ΔH_2 (kJ/mole)	ΔG_2 (kJ/mole)
La_2O_3	−827.4	−433.4	−268.9
Ce_2O_3	−670.1	−400.8	−246.9
Pr_2O_3	−640.0	[b]	[b]
Nd_2O_3	−587.3	−399.6	−235.2
Sm_2O_3	−557.1	−380.2	−215.7
Eu_2O_3	[b]	[b]	[b]
Gd_2O_3	−554.7	−367.4	−198.7
Tb_2O_3	−491.5	[b]	[b]
Dy_2O_3	−498.6	−349.8	−175.6
Ho_2O_3	−475.2	−342.3	−172.3
Er_2O_3	[b]	−321.2	−144.5
Tm_2O_3	[b]	[b]	[b]
Yb_2O_3	[b]	−330.9	−175.3
Lu_2O_3	[b]	[b]	[b]

[a] Reaction 1: $Ln_2O_{3(s)} + 3H_2O_{(v)} + 6CO_{(g)} \rightarrow 2\ Ln(OOCH)_{3(s)}$. Reaction 2: $Ln_2O_{3(s)} + 6CH_3COOH_{(l)} \rightarrow 2\ Ln[OOCCH_3]_{(aq)} + 3H_2O_{(l)}$.

[b] No data available.

It must be emphasized that this is suggested only as an *additional* pathway to those previously proposed, but the different rate dependencies on the concentrations of surface hydrogen, formyl, and formate species could help explain the reported variations in rate and the rate enhancements produced by basic supports. The similarity of this model to previous pathways associated with the interaction of hydrogen with formyl and formate intermediates would not require significant changes in the apparent activation energy. It is apparent that this mechanism would be expected to be important *only* at the Pd–support interface; hence its relative contribution, if any, would depend on the extent of the interfacial region. As mentioned previously there is much evidence that oxide supports, including the REOs, can migrate onto the metal surface during catalyst preparation and pretreatment so that these interface regions can exist on crystallites of any size.

SUMMARY

We have examined the family of lanthanide REO-supported Pd catalysts for CO hydrogenation, measured Pd surface area on fresh and stabilized samples, calculated turnover frequencies for CH_4 and CH_3OH synthesis, and established the trend of these specific activities with the position in the periodic table of the REO support. Although the support clearly influenced the rates of each reaction, different patterns were obtained for methanation at 1 atm and CH_3OH formation at higher pressure. The methanation TOF did not correlate with support acidity, but the 10-fold variation did correlate with the activation energy of electrical conductivity of the REO. We have interpreted this as evidence that electron-deficient cationic sites are created on the support surface which interact with CO adsorbed on Pd to facilitate bond rupture by a redox sequence. The TOF for CH_3OH also varied by an order of magni-

tude and showed a strong correlation with support basicity, as determined by the lanthanide contraction. This again implied a role of the support in this process which, based on results in the literature, seems to be very consistent with a model involving formate intermediates on the support surface. An additional synthesis route which is a heterogeneous analog of the Cannizzaro reaction and could explain the significant rate enhancement obtained with basic supports or by the addition of basic promoters is suggested. The preponderance of activity enhancement in either reaction is expected to be in the metal–support interface region; however, the migration of support oxide species onto the Pd crystallites allows the generation of this interface on large crystallites and obviates the necessity of small crystallites to obtain large interface areas relative to the Pd surface area.

ACKNOWLEDGMENT

This study was sponsored by a grant from Koppers, Inc.

REFERENCES

1. Poutsma, M. L., Elek, L. F., Ibarbia, P. A., Risch, A. P., and Rabo, J. A., *J. Catal.* **52,** 157 (1978).
2. Ryndin, Yu. A., Hicks, R. F., and Bell, A. T., *J. Catal.* **70,** 287 (1981).
3. Sudhakar, C., and Vannice, M. A., *J. Catal.* **95,** 227 (1985).
4. Poels, E. K., van Broekhoven, E. H., van Barneveld, W. A. A., and Ponec, V., *React. Kinet. Catal. Lett.* **18,** 223 (1981).
5. Mitchell, M. D., and Vannice, M. A., *Ind. Eng. Chem. Fundam.* **23,** 88 (1984).
6. Sudhakar, C., and Vannice, M. A., *Appl. Catal.* **14,** 47 (1985).
7. Rosynek, M. P., and Magnuson, D. T., *J. Catal.* **46,** 402 (1977).
8. Touret, D., and Queraux, F., *Rev. Chim. Miner.* **9,** 883 (1972).
9. Palmer, M. B., and Vannice, M. A., *J. Chem. Technol. Biotechnol.* **30,** 205 (1980).
10. Benson, J. E., Hwang, H. S., and Boudart, M., *J. Catal.* **30,** 146 (1973).
11. Yates, D. J. C., and Sinfelt, J. H., *J. Catal.* **8,** 348 (1967).
12. Weisz, P. B., *Z. Phys. Chem. NF* **11,** 1 (1957).
13. Vannice, M. A., *J. Catal.* **37,** 449 (1975).
14. Hicks, R. F., Yen, Q.-J., and Bell, A. T., *J. Catal.* **89,** 498 (1984).
15. Freeman, M., M.S. thesis, Pennsylvania State University, in preparation.
16. Fleisch, T. H., Hicks, R. F., and Bell, A. T., *J. Catal.* **87,** 398 (1984).
17. Chan, S. S., and Bell, A. T., *J. Catal.* **89,** 433 (1984).
18. Hicks, R. F., and Bell, A. T., *J. Catal.* **91,** 104 (1985).
19. Vannice, M. A., *J. Catal.* **40,** 129 (1975).
20. Wang, S. Y., Moon, S. H., and Vannice, M. A., *J. Catal.* **71,** 167 (1981).
21. Berube, M. N., Sung, B., and Vannice, M. A., *Appl. Catal.* **31,** 133 (1987).
22. Rieck, J. S., and Bell, A. T., *J. Catal.* **100,** 305 (1986).
23. Rieck, J. S., and Bell, A. T., *J. Catal.* **103,** 46 (1987).
24. Fajula, F., Anthony, R. G., and Lunsford, J. H., *J. Catal.* **73,** 237 (1982).
25. Ichikawa, S., Poppa, H., and Boudart, M., *J. Catal.* **91,** 1 (1985).
26. Mori, T., Masuda, H., Imai, H., Miyamoto, A., Hasebe, R., and Murakami, Y., *J. Phys. Chem.* **87,** 3648 (1983).
27. Vannice, M. A., *Catal. Rev. Sci. Eng.* **14,** 153 (1976).
28. Ponec, V., *in* "Coal Science," Vol. 3, p. 1. Academic Press, New York, 1984.
29. Rieck, J. S., and Bell, A. T., *J. Catal.*, in press.
30. Bracey, J. D., and Burch, R., *J. Catal.* **86,** 384 (1984).
31. Vannice, M. A., and Sudhakar, C., *J. Phys. Chem.* **88,** 2429 (1984).
32. Ichikawa, M., *CHEMTECH* **12,** 674 (1982).
33. Rabo, J. A., Risch, A. P., and Poutsma, M. L., *J. Catal.* **53,** 295 (1978).
34. Rieck, J. S., and Bell, A. T., *J. Catal.* **96,** 88 (1985).
35. Cotton, F. A., and Wilkinson, G., "Advanced Inorganic Chemistry," 2nd ed. Interscience, New York, 1966.
36. Jiang, X.-Z., Hayden, T. F., and Dumesic, J. A., *J. Catal.* **83,** 168 (1983).
37. Bogoroditskii, N. P., Pasnykov, V. V., Basili, R. R., and Volokobinskii, I. M., *Dokl. Akad. Nauk SSSR* **160,** 578 (1965).
38. Blumenthal, R. N., Lee, P. W., and Panlaner, R. J., *J. Electrochem. Soc.* **118,** 123 (1971).
39. Resasco, D. E., and Haller, G. L., *J. Catal.* **82,** 279 (1983).
40. Cairns, J. A., Baglin, J. E. E., Clark, G. J., and Ziegler, J. R., *J. Catal.* **83,** 301 (1983).
41. Sadeghi, H. R., and Henrich, V. E., *J. Catal.* **87,** 279 (1984).
42. Ko, C. S., and Gorte, R. J., *Surf. Sci.* **161,** 597 (1985).
43. Kelly, K. P., Tatsumi, T., Vematsu, T., Driscoll, D. J., and Lunsford, J. H., *J. Catal.* **101,** 396 (1986).

44. Hicks, R. F., and Bell, A. T., *J. Catal.* **90,** 205 (1984).
45. Driessen, J. M., Poels, E. K., Hindermann, J. P., and Ponec, V., *J. Catal.* **82,** 26 (1983).
46. Ramaroson, E., Kieffer, R., and Kiennemann, A., *J. Chim. Phys.* **79,** 759 (1982).
47. Kikuzono, Y., Kagami, S., Naito, S., Onishi, T., and Tamaru, K., *J. Chem. Soc. Faraday Discuss.* **72,** 135 (1981).
48. Naito, S., Yoshioka, H., Orita, H., and Tamaru, K., "Proceedings, 8th International Congress on Catalysis, Berlin, 1984," Vol. III, p. 207. Dechema, Frankfurt-am-Main, 1984.
49. Hindermann, J. P., Kiennemann, A., Chakor-Alami, A., and Kieffer, R., "Proceedings, 8th International Congress on Catalysis, Berlin, 1984," Vol. II, p. 163. Dechema, Frankfurt-am-Main, 1984.
50. Poels, E. K., Koolstra, R. B., Geus, J., and Ponec, V., "Metal–Support and Metal Additive Effects in Catalysis" (B. Imelik *et al.*, Eds.), p. 233. Elsevier, Amsterdam, 1982.
51. Joyner, R. W., McCarroll, J. J., and Tennison, S., E.P. 101,645, assigned to the British Petroleum Co., 1984.
52. Deligianni, H., Mieville, R. L., and Peri, J. B., *J. Catal.* **95,** 465 (1985).
53. Palazov, A., Kadinov, G., Bonev, Ch., and Shopov, D., *J. Catal.* **74,** 44 (1982).
54. Stupfler, R., Deluzarche, A., Kieffer, R., and Kiennemann, A., *C_1 Mol. Chem.* **1,** 179 (1985).
55. Meriaudeau, P., Dufaux, M., and Naccache, C., "Proceedings, 8th International Congress on Catalysis, Berlin, 1984," Vol. II, p. 185. Dechema, Frankfurt-am-Main, 1984.
56. Hattori, H., and Wang, G., "Proceedings, 8th International Congress on Catalysis, 1984," Vol. III, p. 299. Dechema, Frankfurt-am-Main, 1984.
57. Hicks, R. F., Yen, Q.-J., Bell, A. T., and Fleisch, T., *Appl. Surf. Sci.* **19,** 315 (1984).
58. Ichikawa, M., *Shokubai* **21,** 253 (1979).
59. Moeller, T., "The Chemistry of the Lanthanides," p. 24. Reinhold, New York, 1963.
60. Jackson, N. B., and Ekerdt, J. G., *J. Catal.* **101,** 90 (1986).
61. He, M.-Y., and Ekerdt, J. G., *J. Catal.* **87,** 381 (1984).
62. Ichikawa, M., and Shikakura, K., "Proceedings, 7th International Congress on Catalysis, Tokyo, 1980," p. 925. Elsevier, Amsterdam, 1980.
63. Plyushchev, V. E., Shklover, L. P., Shkol'nikova, L. M., Kuznetsova, G. P., and Nadezhdina, G. V., *Dokl. Acad. Nauk SSSR* **160,** 366 (1965).
64. NBS Tables of Chem. Thermo. Prop., *J. Phys. Chem. Data* **11**(Suppl. 2) (1982).
65. Subba Rao, G. V., Ramdas, S., Mehrotra, P. N., and Rao, C. N. R., *J. Solid State Chem.* **2,** 377 (1970).